Large-Area Electronics: A Platform for Next-Generation Human-Computer Interfaces

Josue Sanz-Robinson, Tiffany Moy, Liechao Huang, Warren Rieutort-Louis, Yingzhe Hu, Sigurd Wagner, James C. Sturm, and Naveen Verma

***Abstract*— Large-area electronics (LAE) is a compelling platform for developing the next generation of human–computer interfaces (HCIs). These systems aim to provide natural interfaces that do not rely on the user providing active and explicit inputs. Instead, user intentions should be inferred implicitly from our natural interactions with the environment and with each other, in order to derive inputs. This requires a large number of sensors to detect signals from interactions and signal-processing to infer the intentions. LAE is a well-suited technology for creating the sensors, enabling these to be diverse and distributed but also conformal. This eases integration in/on environmental and personal surfaces. In order to address the signal-processing required, as well as the other system functions, we develop hybrid LAE/CMOS architectures, which exploit the complementary strengths of the two technologies. We demonstrate the hybrid architectures in several testbed systems, and focus on two of these as case studies: 1) A source separation system, which uses a large-area microphone array to separate the voice of multiple simultaneous speakers in a room; 2) An electroencephalogram (EEG) acquisition and biomarker-extraction system based on flexible, thin-film electronics.**

***Index Terms*— a-Si, electroencephalogram (EEG), human–computer interfaces (HCIs), hybrid system, large-area electronics (LAEs), source separation, TFT.**

I. Introduction

THOUGH we have seen tremendous advancement in the computational capabilities of electronic systems, we have not seen a proportionate rise in natural interfaces whereby such capabilities can be seamlessly accessed while we live, work, and play. Indeed, progress has been made towards more natural ways of interfacing with electronic systems, such as touch screens in consumer devices; however, these require users to actively and explicitly provide inputs, thus disrupting our natural activities. This restricts the scenarios in which we can or would like to use such systems. Our vision for the next generation of human–computer interfaces (HCIs) consists of sensors that are integrated into our everyday lives, and which do not rely on our explicit inputs, but instead are able to infer our intentions from our interactions with our environments and with each other. Such HCIs do not need us to turn our attention away from our natural activities, thereby expanding the ways and scenarios in which we can make use of electronic systems. We identify two critical attributes of such HCIs: 1) the ability to opportunistically detect human-activity and -interaction signals, through a large number of distributed embedded sensors; and 2) the ability to perform inferences over the acquired signals, through advances in embedded computing and algorithms, in order to determine how and what services should be deployed by electronic systems.

Fig. 1. An example of HCIs for ambient sensing.

As illustrated in Fig. 1, when we physically interact with the environment and each other, we produce a plethora of signals, such as pressure when we speak or touch objects, radiated heat from our bodies, carbon dioxide when we exhale, varying electrostatic fields when we move with respect to objects, and biopotentials caused by physiological processes in our bodies (e.g., nervous, skeletal-muscular, cardio-vascular systems). Given the diverse types and locations of human-activity/ interaction signals, and the diverse features these may provide for inferring intentions, traditional technologies for sensing (e.g., discrete-point sensing nodes and remote sensing nodes [1]) are likely to limit our ability to achieve the HCIs envisioned. Thus, as a starting-point technology for creating such HCIs, we turn our focus to a technology called Large-Area Electronics (LAE). LAE is based on low-temperature processing of thin films. This enables compatibility with diverse materials, leading to a broad range of transducers (for sensing and energy harvesting) which can be fabricated on substrates such as glass and plastic, for large ($> 1\ m^2$) and highly-flexible form factors [2]. This make LAE a potential platform for creating diverse sensors distributed over a physically-

Manuscript received May 17, 2016; revised August 4, 2016; accepted September 27, 2016. Date of publication November 22, 2016; date of current version March 15, 2017. This paper was recommended by Guest Editor J. S. Chang.

The authors are with the Department of Electrical Engineering, Princeton University, Princeton, NJ 08544 USA (e-mail: sanzrobinson@gmail.com).

Color versions of one or more of the figures in this paper are available online at http://ieeexplore.ieee.org.

Digital Object Identifier 10.1109/JETCAS.2016.2620474

expansive space, and it also enables dense spacing of sensors for high-resolution of measurements. Furthermore, its flexible and lightweight form-factor, with substrate thicknesses of one-to-one hundred μm [3], facilitates the deployment of sensors unobtrusively in a wide variety of scenarios, ranging from the walls of a room, to the wings of an aircraft, to the body of a person. Over the last 15 years, a wide variety of such sensors have been demonstrated, including strain [4], light [5], gas [6], pressure [7], biopotential [8], etc.

However, while transformational for enabling the sensing required for HCIs, we note that LAE is inadequate for creating full systems. This because low-temperature processing leads to transistors with orders-of-magnitude lower performance and energy efficiency than traditional transistors available in silicon-CMOS integrated circuits (ICs). Most importantly, this limits the ability to derive advanced inferences from the acquired signals, as required of the HCIs. Thus, in this paper we focus on *hybrid systems*, which combine LAE with silicon-CMOS ICs [9]. We describe the generalized structure of hybrid-system platforms, but we place specific emphasis on the specialized algorithms these require for extracting specific outputs, leading to user intentions or states that can drive automatic responses from electronic systems. We do this in the context of two classes of HCIs, for which LAE is critically enabling: 1) ambient HCIs based on sensing our interactions with our environments, by exploiting large-area, diverse sensing distributed across the length scales of our environments, and 2) on-person HCIs based on sensing physiological signals, by exploiting light-weight, highly-conformal sensing worn with minimal obtrusiveness on the body.

The remainder of the paper is organized as follows. Section II motivates hybrid systems, presenting generalized principles and architectures for the platforms, derived from previous experimental demonstrations. To concretely examine the translation of such platforms to specific HCIs, we note that especially the signal-inference/-processing algorithms are largely driven by specific characteristics of the applications. Thus, we present two case studies corresponding to the two classes of HCIs (ambient and on-person HCIs). Section III describes a system for separating the voices of two simultaneous speakers, based on the spatial-filtering capability of a large-area, thin-film microphone array [10], [11]. Section IV describes an electroencephalogram (EEG) acquisition and biomarker-extraction system based on flexible, thin-film electrodes [12]. In both sections, the focus is on the systems and algorithms aspects, and details of the circuit and architectural designs are provided in the respective references cited. Finally Section V concludes.

II. Hybrid Systems for HCIs

As Section I states, the hybrid approach is required to exploit the transformational sensing capabilities of LAE in practical systems. Namely, complete systems require sensors and energy harvesters to be combined with functionality for instrumentation, computation, power management, and communication. While LAE does enable the creation of thin-film transistors (TFTs) which could implement such functions, low-temperature processing, which is required for forming diverse and expansive sensor arrays, leads to low performance. For illustration, Table II shows transistor parameters for two LAE technologies we fabricate in house [amorphous-silicon (a-Si) TFTs and zinc-oxide (ZnO) TFTs], compared with a foundry crystalline-silicon (c-Si) CMOS technology. Thus, to realize the required functionality efficiently and on a scale that can exploit the level of sensing possible in LAE, a high-performance transistor technology such as c-Si CMOS is required. However, in hybrid systems, the use of disparate technologies raises distinct challenges, specifically around interfacing signals between the two domains. This drives the design of specialized architectures for the various functions required [9].

TABLE I
Comparison of Transistor Performance

	a-Si	ZnO	c-Si (130 nm)
Processing Temperature ($^\circ C$)	180-350	200	1000
Bi- / uni-polar	Only n-type	Only n-type	Both n-type and p-type
Field Effect Mobility (cm^2/Vs)	μ_e=1 μ_h=0.05	μ_e=20	μ_e = 1000 μ_h = 500
Unity-Gain Cutoff Frequency (f_t)	1 MHz	5-10 MHz	150 GHz

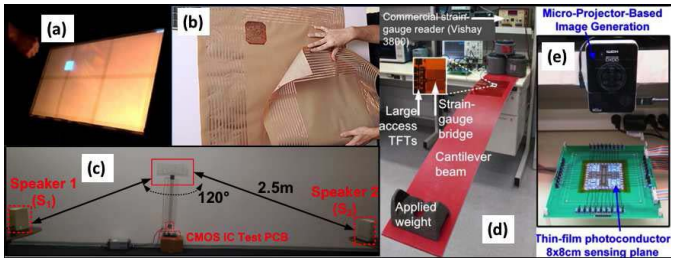

Fig. 2. Examples of hybrid systems, including (a) gesture sensing [13], (b) array of radio front-ends [17], (c) voice sensing [10], (d) strain sensing [15], and (e) image detection [14].

Thus, to concretely understand platform architectures for hybrid systems, our research has developed a number of such systems, some of which are depicted in Fig. 2. A few examples include the following (with circuits and systems details in the provided references):

- 3D gesture-sensing based on extended-range capacitive sensing [13].
- Voice sensing to enhance human speech in loud environments and act as a front-end for a voice-command recognition engine [10], [11].
- Electroencephalogram (EEG) sensing with a flexible form-factor to improve patient comfort, and with signal processing for seizure detection [12].
- Large-area imagers, which carry out object classification using embedded machine-learning classifiers [14].
- Strain sensing to monitor civil infrastructure and detect early-stage cracks for structural-health monitoring [15], [16].
- Distributed, flexible array of radio front-ends based fully on TFTs for lining walls of a space to communicate with distributed sensors [17].

TABLE II
EXPLOITING THE COMPLEMENTARY STRENGTHS OF CMOS AND LAE

	CMOS	LAE
Sensors	Precision instrumentation and digitization.	Wide variety of thin-film sensors, depositable on large, flexible substrates.
Communication	Physical-layer transceivers.	Low-loss interconnects for telemetry.
Power	Power management circuits.	Large devices for harvesting substantial power.
Computation	High-performance and energy-efficient transistors.	WEAKNESS: Modest-performance and non-complementary transistors.

Insights gained from these systems have resulted in generalized principles as well as platform architectures, circuits, and devices for hybrid systems. On a high level, the distribution of functionality between the LAE and c-Si CMOS domains, across the various sub-systems required, follows directly from the complementary respective strengths of the two technologies. This distribution is summarized in Table II. However, as mentioned, more specifically, practical hybrid systems are limited by the interfacing of signals between the two technology domains. Thus, this becomes a primary driver of many design choices associated with the sub-systems and complete systems. Details and analyses of the architectural design choices are provided in [9], while details and analyses of the physical design choices (e.g., assembly of multi-sheet hybrid systems) are provided in [3].

Generally, we find that many approaches taken for the platform architectures can be fairly generic across applications (for control, noise-management, modulation, multiplexing, and transfer of domain-crossing signals). On the other hand, we find that the systems algorithms required, tend to be more strongly associated with the specific applications; yet, in many cases, important aspects of the algorithms are also driven by attributes and limitations (most notably interfacing) of the hybrid-system platform. For the HCIs envisioned, system algorithms are of particular importance, given that the sensed signals only weakly and/or indirectly provide features for inferring human intentions. With previous publications from our group focusing on the platform architectures and physical design [9], [3], the remainder of this paper focuses on the systems algorithms for HCIs. Due to the stronger association these have with applications, we present the algorithmic approaches through two case studies, representing ambient and on-person HCIs. While experimental demonstrations of these have been previously reported [10], [12], here we focus on the systems algorithms, specifically highlighting two critical aspects:

1) The envisioned HCIs place an emphasis on advanced signal processing in order to translate raw sensor signals into inferences about human intentions. In particular, the inferences are based on features derived from diverse signals, which only peripherally express how we would like embedded computing systems to provide services. Thus, how sensed signals correlate with both the features and the inferences may be complex.
2) Hybrid systems face several specific platform challenges, especially due to the low performance and/or non-ideal behavior of LAE functions. Signal processing gives us system-level solutions for overcoming these, which we often find to offer significantly greater leverage and designer flexibility than technology-level solutions. For example, as we will show, signal processing enables sensor variations and the number of interconnects from large-area sensors to be mitigated, which are two key considerations for large-scale hybrid systems.

III. CASE STUDY 1: BLIND AUDIO-SOURCE SEPARATION FOR AMBIENT SENSING

Ambient electronics has the potential to foster collaborative spaces and enhance interpersonal interactions. LAE is a promising technology for these systems, since they require a flexible form factor, to enable deployment, but also must readily support large numbers of spatially-distributed sensors. For example, when designing a control system for heating a room, a single isolated temperature sensor is sub-optimal, since it provides no information about the temperature gradient or the microclimate in the room. Therefore, there is insufficient information to determine which heaters or circulation fans should be turned on or off, so as to obtain the desired room conditions and reduce energy usage. Similarly, a gesture sensing system for a large display needs electrodes that are spatially distributed over meters, since not only can a single hand-gesture span close to a meter, but a user can also gesture at different locations on the screen [13]. As a vehicle to explore ambient-sensing systems, we designed a system for separating the voices of multiple simultaneous speakers, which can ultimately be fed to a voice-command recognition engine for controlling electronic systems. Circuit and architectural details are provided in [10].

A. System Overview

A key attribute for ambient-sensing systems, such as this one, is exploiting diversity in the types of interactions and activities users present across the spaces they inhabit. Thus, spatially-distributed sensing and signal processing to exploit the resulting spatial diversity is a primary focus. Fig. 3 shows an overview of our source separation system [10], [11]. In the large-area domain the system consists of a 16-element microphone array, spanning 2.25 m, which has been attached to a wall of a conference room. Flexible microphones made from polyvinylidene fluoride (PVDF), a piezoelectric polymer, and localized TFT amplifiers have been developed. The signals from the amplifiers are subsequently fed to a CMOS IC for system control, sensor readout and digitization. On a signal-processing level we developed an algorithm for source separation, based on beamforming. A key feature of this algorithm is that it is "blind", e.g., it requires no knowledge about the location of the speakers or microphones, but instead

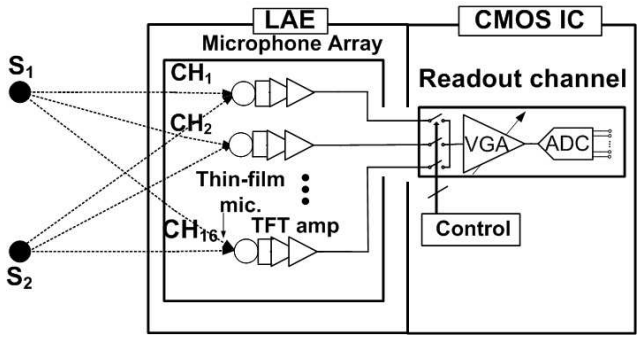

Fig. 3. System architecture of a source separation system based on a large-area microphone array.

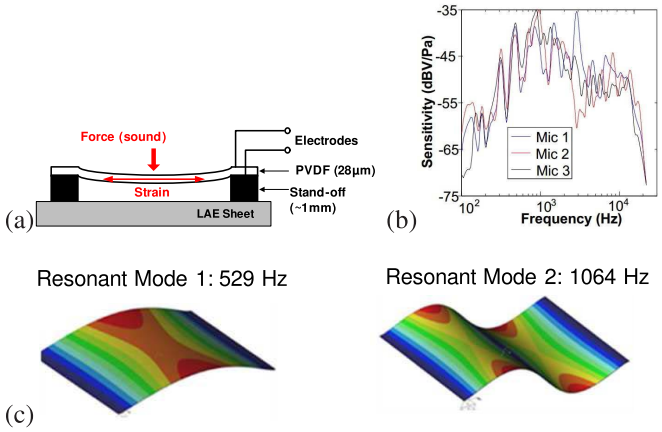

Fig. 4. Thin-film PVDF microphone design, including (a) structure, (b) frequency response (measured in an anechoic chamber, with a loudspeaker directly facing the microphone), and (c) finite element simulations showing the resonant modes [10].

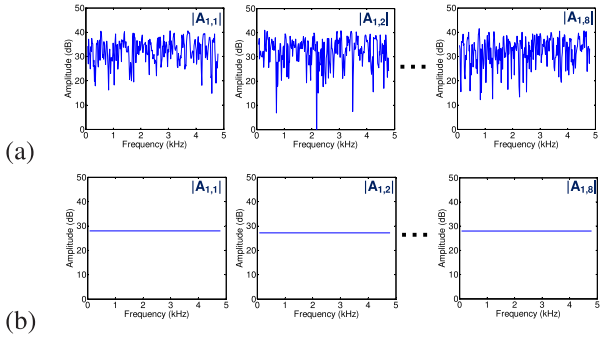

Fig. 5. Simulated frequency response of perfectly uniform, omnidirectional microphones and speakers in a (a) reverberant room, and (b) non-reverberant room [10].

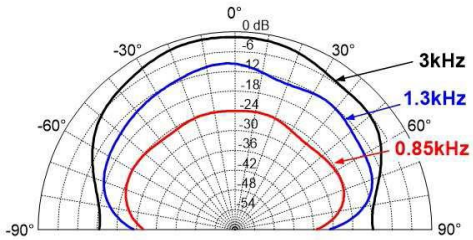

Fig. 6. Polar diagram measured in an anechoic chamber of a PVDF microphone [10].

it adapts to the unique acoustic environment of the room. Specifically, it has been designed to work in reverberant rooms, such as the majority of rooms found in a typical building, and it can support the wide variations associated with large-area microphones.

1) Sensors: PVDF Microphone: As shown in Fig. 4, the microphone we developed has a diaphragm made from PVDF, a piezoelectric thin-film polymer, which is attached to two standoffs, so as to form a bridge-type structure. The microphone is a pressure-gradient microphone. This means that since it is not inside a sealed enclosure, the diaphragm deflects due to a pressure difference between the sound reaching the top and bottom face [18]. Mechanical-to-electrical transduction functions primarily in the piezoelectric d_{31} mode, where it converts horizontal strain into a vertical potential difference between the electrodes.

The PVDF is 28 μm thick, and has dimensions of 1.5 cm (width) $\times$ 1.0 cm (length). These dimensions were chosen to ensure that the microphone was exposed to a uniform sound field, since the wavelength ($\sim$ 7 cm) for the maximum frequency of interest for speech (5000 Hz) is substantially larger than the microphone. As shown in Fig. 4, due to its bridge-type structure, the microphone has numerous resonant peaks. We have tuned the strain of the PVDF diaphragm to match the resonant peaks of human speech, which is concentrated from 500–3000 Hz [19].

When developing a system based on a large-area microphone array it is important to take into account that the frequency response of the microphones to a single speaker varies significantly. This can be attributed to:

1) Location in the room: When sound is traveling from a speaker to a microphone it experiences significant reverberations (reflections) from surfaces in the room. For example, Fig. 5(b) shows the simulated frequency response for a microphone with a perfectly flat frequency response in an room with no reverberations (e.g., anechoic), while Fig. 5(a) shows the frequency response for the same microphone in a typical reverberant room. This is one of the principal sources of variation and cannot be tackled by improving the microphone. Instead circuits and algorithms need to be designed that are robust to microphone variation.
2) Manufacturing variability: During manufacturing microphone parameters, such as the tension of the diaphragm, can vary. Fig. 4(b) shows the frequency response of three microphones that were fabricated using the same process. Although improvements in the manufacturing process could reduce this variation, the large-area nature of the processing means a significant level of variation is likely to remain.
3) Microphone directionality: Since the microphone is a pressure-gradient microphone, different sound pressures act on both faces of the PVDF diaphragm depending on the direction of sound, causing a directional frequency response (see Fig. 6).

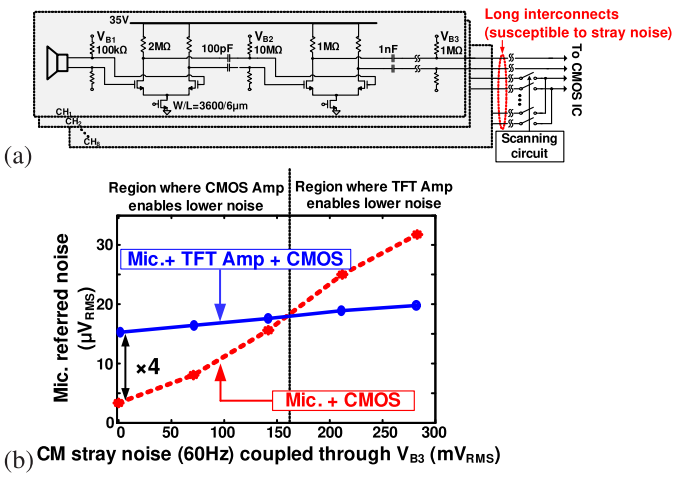

Fig. 7. (a) Schematic of a two stage TFT amplifier, including (b) the simulated tradeoff between including versus not including a localized TFT amplifier before long interconnects to a CMOS IC [10].

2) Pre-Amplifiers–Localized LAE versus Centralized (CMOS-IC) Amplifiers: For this system one of the key tradeoffs is whether to amplify the signal from the microphone using LAE, TFT-based amplifiers or to amplify it directly on the CMOS IC. The TFT-based amplifiers have the advantage of being localized, since they are fabricated directly adjacent to the microphone. On the other hand the CMOS IC amplifiers benefit from having transistors with lower noise and better power efficiency for a target noise level, but have long interconnects ($\sim$ 1 m) between the LAE microphone and the CMOS IC, which are susceptible to stray noise coupling.

When comparing these options we implemented both a localized TFT-based amplifier, and a low-noise amplifier (LNA) on the centralized CMOS IC with $\sim$1 m long interconnects. The thin-film amplifier consists of a two-stage differential amplifier, formed from a-Si TFTs [20] with W/L=3600 μm/6 μm, as shown in Fig. 7. The first stage is a gain stage (with gain of 17 dB), while the second is a buffer stage (with gain of 3 dB) to drive long ($\sim$ 1 m) interconnects from the LAE to the CMOS IC. The LNA on the CMOS IC consists of a single-stage resistively loaded differential amplifier. In order to achieve the low noise performance, a relatively large-sized input transistor (96 μm/12 μm) is employed to reduce the $1/f$ noise. The LNA is designed to have a gain of 16 dB with 2.6 μV_{RMS} integrated noise between 0.3 and 3 kHz.

To analyze the noise tradeoff, common-mode noise at 60 Hz is intentionally coupled to the differential LAE interconnects preceding the CMOS IC (through the bias node V_{B3}, see Fig. 7). When no noise is coupled, the remote CMOS amplifier has 4$\times$ lower total input referred noise than the localized LAE amplifier. This is due to the noise of the TFT amplifier itself. However, with a stray noise of just 160 mV, which is a value typically exceeded for certain microphone channels during testing, the TFT amplifier has an input referred noise lower than the CMOS. This highlights the benefit of using localized LAE amplifiers fabricated over large-areas to interface with the microphones.

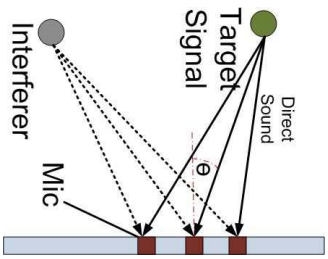

Fig. 8. Sound propagating from two simultaneous sources to a microphone array in an anechoic room.

3) CMOS IC: As shown in Fig. 3, the output of the LAE amplifier is fed into a Variable Gain Amplifier (VGA) on the CMOS IC. The VGA plays a key role by compensating for sensitivity variations and, in turn, the widely differing amplitudes of the signals outputted by the thin-film microphones. Following the VGA there is an integrating ADC, which digitizes the sample to 11 bits [10].

B. Signal Processing: Beamforming-based Blind Source Separation

1) Background - Beamforming in an Ideal Room: Delay-and-sum beamforming uses a microphone array to "focus" on a given source. Therefore, it can be used to enhance a target sound source, and cancel undesired sources, known as interferers.

As shown in Fig. 8, since the array can be treated as a linear system, each microphone receives a summation of the target signal to be recovered and the interferer. In an anechoic room (e.g., with no reverberations), the difference in the time it takes for the sound from a given source to reach two microphones, known as the time difference of arrival (TDOA), is the same for all frequencies. Assuming the source is in the far-field, so sound can be treated as a planar wave, the difference in TDOAs between a pre-selected reference microphone and another microphone, m, for a source, s, can be calculated using a simple geometric expression

$$D_{ms} = \frac{d \sin(\Theta)}{c} \tag{1}$$

where d is the microphone spacing, c is the speed of sound in air, and Θ is the angle between a microphone and the source.

In conventional delay-and-sum beamforming, the already known TDOAs are used to time align the target signal across all microphones in the array, so they add constructively. At the same time the interferer will be attenuated preferably, due to it adding incoherently. The output of a conventional delay-and-sum beamformer when "focusing" on a source, s, can be expressed as [21]:

$$\widehat{x'}^{s}(t) = \sum_{m=1}^{M} y_m(t - D_{ms}) \tag{2}$$

where $y_m(t)$ is the signal recorded at each microphone, m, and consists of the sum of the time delayed target signal and the interferer.

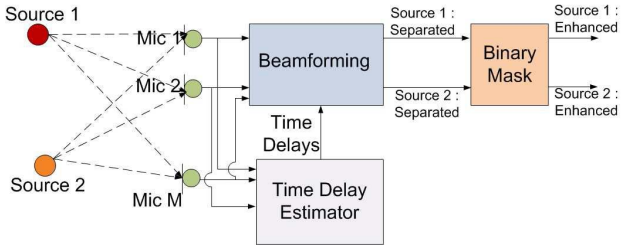

Fig. 9. Block diagram of source separation algorithm.

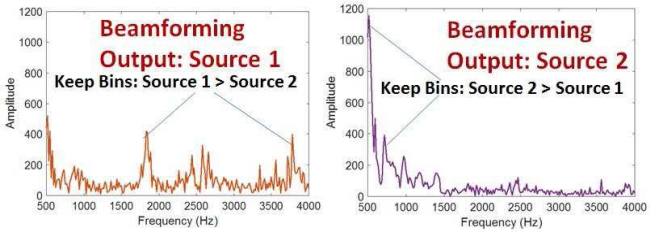

Fig. 10. Applying a binary mask to a time frame outputted by the beamforming stage.

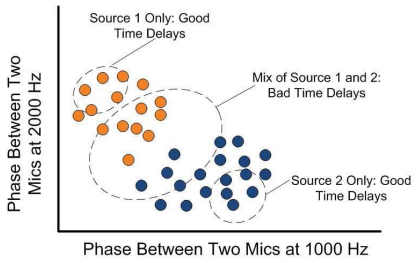

Fig. 11. Cluster analysis applied to different frames (represented by points) to identify a frame where only one source is active.

2) Algorithm Design—Beamforming in a Reverberant Room: In a practical room conventional delay-and-sum beamforming is not a viable approach for source separation. This is due to reverberations from surfaces leading to multipath propagation, causing the time delays between microphones to be frequency dependent and difficult to estimate using a geometrical expression [22], particularly in the presence of the strong directionality exhibited by the PVDF microphone structure. To overcome these challenges we developed an algorithm that makes no assumptions about the propagation of sound in the room. Rather, we extract time delays for each microphone-source pair on the fly from the sound mixture of simultaneous sources. This enables our algorithm to adapt to the unique acoustic properties of each room (e.g., size, reverberation time, placement of objects), changes in locations of the sources, and variations (directionality) in microphone transduction. The algorithm is "blind", because it requires no information about the location of speakers or sources. The only information our algorithm needs about the environment is the number of sources. Thus, we avoid time consuming and technically challenging location measurements [23].

As shown in Fig. 9, the algorithm consists of a beamforming, binary mask and time delay estimator stage. The beamforming stage uses the same principles as conventional delay-and-sum beamforming, given by (2). It differs by being implemented in the frequency domain, so as to utilize frequency-dependent time delays. The frequency-domain output of the beamformer for a frame with index, L, can be expressed as

$$\widehat{X}'^{s}_{ref}(\omega, L) = \sum_{m=1}^{M} Y_m(\omega, L) e^{-j\omega \mathrm{D}_{ms}(\omega)} \tag{3}$$

where $Y_m(\omega, L)$ is the mixture recorded by each microphone, and $D_{ms}(\omega)$ is the frequency-dependent time delay between the reference and each microphone.

Due to the wide dynamic range of human hearing, we found that the beamforming stage alone did not sufficiently cancel out the interferers. Therefore, we implemented an additional binary mask stage. This stage exploits the fact that when speech is represented in the frequency domain, for short time frames (~100 ms) the frequency bins with the largest magnitude from one speaker rarely overlap with the frequency bins with the largest magnitude from another speaker [24]. To further cancel interferers we can compare the separated output for one speaker with the separated output for another speaker after the beamforming stage. If a given bin is larger for one speaker than the other speaker, we keep the bin, otherwise the bins is set to zero. This operation is illustrated in Fig. 10.

To estimate the frequency dependent time delays, one option is to carry out a calibration procedure before running the separation algorithm. The procedure is based on extracting the time delays from a segment of speech with each speaker talking in isolation. To avoid this calibration procedure, we instead extract the time delays in the background from the recording with multiple simultaneous speakers, while at the same time running the separation algorithm (e.g., the beamforming and binary mask stage). In this case, we extract the time delays for a given speaker by identifying a short time frame from the recording with multiple speakers in which only one of the speakers is primarily active. We use cluster analysis to identify this frame. As illustrated in Fig. 11, each point is extracted from a different frame of the speech mixture, where the axes (e.g., the feature vector) consists of the phase difference for each frequency bin between two microphones in the array. Each frame is classified, using a k-means algorithm [25], exclusively as belonging to one source or another, even if the frame consists of a mixture of multiple sources or contains no speech. Therefore, to identify a frame where only one source predominates, for each point from a given cluster we calculate the Silhouette Factor, which is a statistical measure of how well a point belongs to the cluster, based on minimizing intra-cluster distances and maximizing inter-cluster distances [26]. The frame from each cluster with the largest Silhouette Factor is used to estimate the time delays.

C. System Demonstration

To test our system, we used two simultaneous speech recordings played through two loudspeakers. The experiment was setup in a reverberant conference room, as shown in Fig. 12. To characterize the quality of our algorithm we used

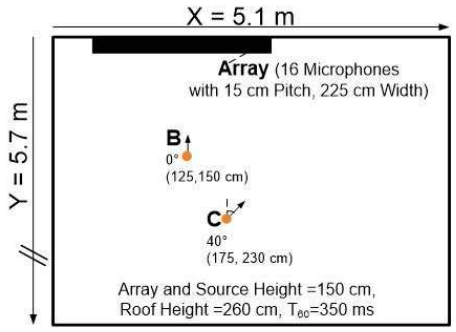

Fig. 12. Experimental room setup (top view). Experimental room setup (top view). Drawn to scale. B and C are the speakers located at coordinates (x,y), with speaker orientation given by the angle accompanying each source. T_{60} is the room reverberation time. [11].

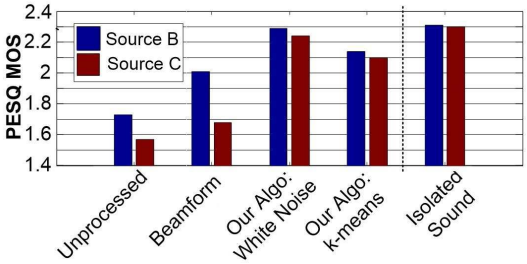

Fig. 13. Separating two sources with an array of LAE (PVDF) microphones [11].

the Perceptual Evaluation of Sound Quality (PESQ) metric, with clean speech recordings from the TSP database [27] as the reference signal. PESQ mean opinion scores (MOS) range from -0.5 (bad) to 4.5 (excellent) [28]. As shown in Fig. 13, we obtained high quality separation results for the PVDF microphone array, which were only slightly lower than the PESQ scores that would be obtained if one of the sources were to played in isolation (e.g., the best possible PESQ score). When we only used the beamforming stage with frequency dependent time delays, but not the full algorithm including the binary mask stage, results were much poorer, which demonstrates the need for this mask stage. Additionally, we compared the results obtained when extracting time delays from recordings with both speakers talking simultaneously (e.g., using the k-means time delay estimator) and when using white noise played by each speaker in isolation. The scores using the time delay estimator were only slightly lower, showing the effectiveness of our time delay estimator stage. We also carried out critical listening tests using two live, simultaneous human speakers. For these experiments we also obtained high quality separation results, but cannot report PESQ scores, since they cannot be calculated for this scenario.

To explore the impact of the microphone on the performance of our algorithm, we repeated the same experiment using commercial electret condenser microphones (EM-172 capsules from Primo Inc.), as shown in Fig. 14. In this case the same trends were observed as with PVDF microphones, but the PESQ scores were larger due to the increased sensitivity and flatter frequency response of the condenser microphones. This highlights the value of further improving

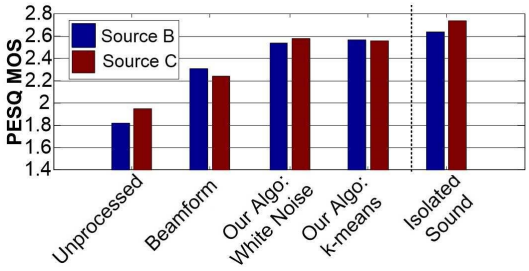

Fig. 14. Separating two sources with an array of electret microphones [11].

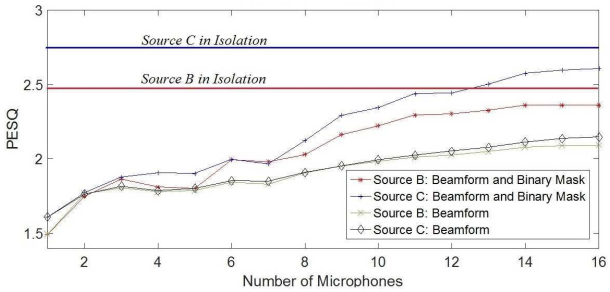

Fig. 15. Algorithm performance as function of the number of microphones, experimentally measured with two sources and electret microphones.

the thin-film microphone, including carrying out research on alternative piezoelectric thin-film materials that could lead to higher sensitivity microphones, such as Macro Fiber Composites (MFC) [29].

Two aspects of importance when considering LAE as a technology for achieving spatially-distributed sensing is how system performance is impacted by microphone non-idealities and element scaling, both possibilities arising due to the use of LAE. To explore the impact of non-idealities on the performance of the system, we tested our algorithm on arrays with different numbers of microphones (Fig. 15). Initially, when we incrementally added microphones the PESQ score improved rapidly, but with many microphones the PESQ score started to level off. This result suggests that for our experimental setup, there is a logarithmic relationship between the number of microphones and the signal-to-interferer ratio, as predicted by beamforming theory [30], [31]. Nevertheless, to obtain satisfactory separation results we require at least 10 microphones, demonstrating the need for arrays that span large-areas. Similarly, we found that to obtain satisfactory separation results, for an array with 16 microphones, we required an inter-microphone spacing of at least 10 cm. A possible explanation is that for small microphone spacing, the interferers after beamforming are not uncorrelated, which is detrimental for the algorithm.

IV. Case Study 2: EEG Acquisition System for On-Person Sensing

On-person sensing systems provide an unprecedented ability for human users to continuously monitor and obtain closed-loop feedback about their physiological condition, enabling diverse applications such as observing bodily functions during

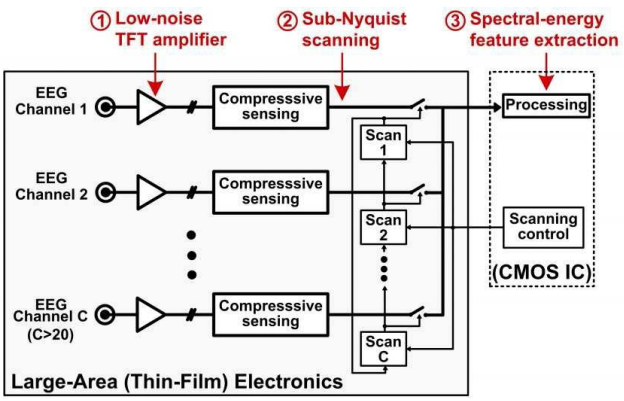

Fig. 16. System architecture for the EEG acquisition and biomarker-extraction system, where LAE circuits interface with an eventual CMOS IC [12].

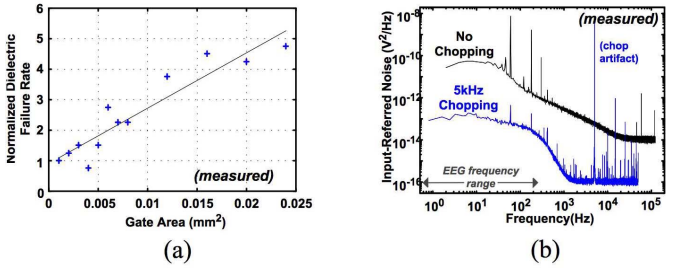

Fig. 17. TFT chopper-stabilized amplifier. (a) Dielectric failure rate as a function of gate area, and (b) effect of the chopper amplifier on the noise power spectral density [12].

physical exercise, watching the health of medical patients, or monitoring the stress signals of emergency professionals [32]. By collating information from a wide variety of individuals over extended periods of time, on-person sensing systems could have a wide-ranging positive impact on human health and quality of life, allowing individuals to gain insight about their own physiology and giving policymakers improved information for taking public health decisions. LAE can play an important role in the development of these systems by providing a platform for building flexible and lightweight sensing systems that can have a form factor that is comfortable and unobtrusive to wear over extended periods of time.

A. System Overview

As a vehicle to explore this application space, we developed an EEG acquisition and biomarker-extraction system with a flexible-form factor. The system aims to overcome the disadvantages of traditional EEG-recording systems, including requiring careful electrode placement on the scalp and needing large amounts of cabling, which reduce patient comfort, especially during long recording sessions, and prevent widespread adoption outside of a clinical setting. A system diagram is shown in Fig. 16, and circuit details are provided in [12]. Similar to the prior case study, this system also emphasizes a hybrid LAE / CMOS architecture, and involves co-designing sensors, circuits and signal processing. For this system, where a typical arrangement might consist of 18 electrodes, and can be have in excess of a hundred electrodes, one of the principal design considerations is to reduce the number of interfaces between the LAE and CMOS domains. This is because the number of interfaces pose a dominating concern for assembly complexity, cost, and reliability. The reduction in interfaces is achieved by combining electrodes and TFT circuits on the same flexible sheet. Not only do the TFT circuits enable signals from multiple electrodes to be multiplexed on the same output interface, but, motivated by limited sampling rate due to speed limitations of the TFT multiplexing circuits, it enables the implementation of compressive-sensing acquisition to reduce the sampling rate requirements. On a signal-processing level, the system aims to not only reconstruct EEG time-domain waveforms, but also extract features of the EEG for a broad range of inferences. In addition to current clinical applications, readily deployable EEG systems are envisioned to enable Brain Computer Interfaces in our daily lives, for applications ranging from detection of mental states [33] to possibly vehicular control [34].

1) TFT Instrumentation Amplifier: A primary challenge with EEG acquisition is the low amplitude of signals (∼10-100 μV). This necessitates localized low-noise amplifiers near the electrodes to mitigate the subsequent influence of stray noise sources. The problem with a TFT implementation is that TFTs have large 1/f noise in the spectral band of interest for EEG acquisition, due to high density of traps in the semiconductor and semiconductor-dielectric interface. A standard approach for addressing 1/f noise is to increase device dimensions. However, while this also works for TFTs, low-temperature-deposited gate dielectrics have increased susceptibility to pin holes, causing the increased failure rate shown in Fig. 17(a). Thus, an alternative employed in the system is the use of a chopper-stabilized amplifier topology [35], where the input signal is first up-modulated to a frequency band less affected by 1/f noise, then amplified, and then down-modulated back to baseband. While this requires the TFTs to operate at higher speed, analysis [12] shows that this is readily achieved, leading to the measured improvement in noise power spectral density (PSD) shown in Fig. 17(b), as required for EEG acquisition.

2) TFT Scanning: As mentioned, a critical design objective for the EEG system is to minimize the number of interconnections to the CMOS IC. This is achieved by multiplexing multiple EEG channels onto a single interface, enabling their accessing sequentially, one at a time. The scanning circuit, shown in Fig. 18, enables us to acquire data from an arbitrary number of LAE sensors through only a single output interface between the LAE and the CMOS IC. It requires only three control signals (two-phase clock signals, CLK/CLKb, and a global reset signal, GRST) from the CMOS IC, which are initially inputted into TFT level converters to generate higher voltage swings. Each channel has its own scanning circuit block, which is connected as a chain to blocks from other channels. The transition of CLK/CLKb is used to sample the blocks in a sequential manner, so that at any given time only one block has access to the interface and all other blocks are disabled [36].

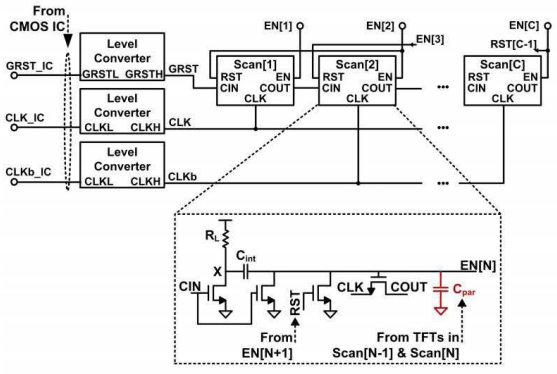

Fig. 18. TFT scanning circuit [12].

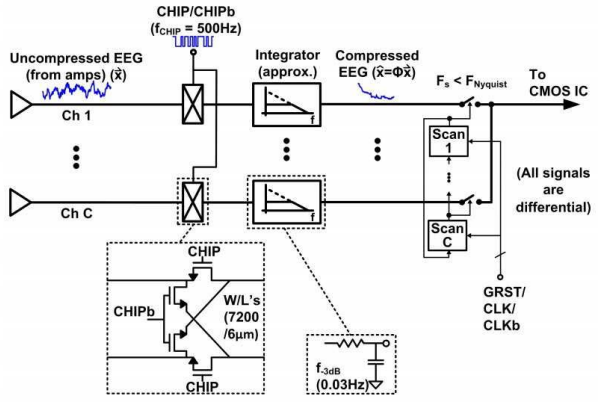

Fig. 19. Compressive-sensing acquisition circuits based on TFTs for sub-Nyquist scanning [12].

The speed of each block within the scanning circuit is limited by a critical time constant set by the load resistor R_L and output capacitor C_{int}. It should be noted that the designer cannot independently select the value of these components, but rather they are ultimately set by the TFTs. Due to the lack of PMOS transistors, the scan block relies on a pseudo-NMOS stage for charging and discharging node X. Thus, for adequate swing, R_L must be large with respect to the on current of the stage TFT. Similarly, when node X rises, the enable signal EN[N] is raised through a capacitor divider formed by C_{int} and the parasitic load capacitances of subsequent TFTs. This means that C_{int} must be sized to be significantly larger than the TFT parasitic capacitances. For a-Si TFTs, this time constant limits the scanning speed to about 10 kHz. While the EEG signals themselves have a bandwidth of about 300 Hz, after passive single-pole filtering of each channel, a bandwidth of 2 kHz is required for robust Nyquist sampling. Thus, the scanning speed would limit the number of channels in the system to less than five. To overcome this limitation we employ compressive-sensing acquisition, as described in Section IV-B.

B. Signal Processing: Compressive Spectral-Energy Feature Extraction for Seizure Detection

1) Background: Traditionally, a signal is acquired by sampling at a rate above the Nyquist rate. Compressive sensing provides an alternative by exploiting sparsity in the signal, possibly when it is represented in some transform domain. EEG signals are known to be sparse in the Gabor domain. This makes compressive sensing well suited for the EEG system, by enabling reconstruction over an increased number of channels to be sampled by the speed-limited scanning circuit.

While our primary interest is in extracting features of the EEG to enable inferences, compressive sensing has been most commonly employed to reconstruct an original signal, represented as a vector $\vec{x}$ of dimensionality N. This is done by expressing the signal as

$$\vec{x} = \Psi \vec{s} \tag{4}$$

where Ψ is known as the representation matrix, consisting of concatenated column vectors corresponding to a basis where $\vec{x}$ is sparse. Thus, $\vec{s}$ is a column vector with dimensionality N, consisting of weighting coefficients. If $\vec{x}$ is indeed sparse, only a small number of elements in $\vec{s}$ will have non-zero value. These can be determined by a corresponding number of measurements taken of $\vec{x}$. The theory of compressive sensing dictates that any set of measurements represented by the M-dimensional vector $\vec{y}$ is adequate, such that

$$\vec{y} = \Phi \vec{x} = \Phi \Psi \vec{s}, \tag{5}$$

where Φ is an $M \times N$ matrix referred to as the measurement matrix, so long as the $\Phi\Psi$ satisfies the Restricted Isometry Property (RIP) [37]. In this case, reconstruction simply requires finding a sparse solution for $\vec{s}$ in (5), which can be done using L1-norm minimization. It should be pointed out that, using a Gabor basis Ψ, with which EEG is known to be sparse, a random matrix Φ will satisfy RIP with high likelihood [38], making the required measurements for sparse reconstruction of EEG rather amenable to acquire.

2) Algorithm Implementation: Instead of reconstructing EEG signals, our interest is in extracting features for performing inferences; and, instead of performing compressive sensing in the discrete digital domain, our interest is in performing compressive sensing in the analog domain before sampling of channels by the speed-limited scanning circuit. First, to perform compressive sensing, we implement an analog architecture [39] in the LAE domain, as shown in Fig. 19. A modulator (shown in the inset) applies a pseudorandom chipping sequence of $\pm$ 1 at 500 Hz, which comes from a CMOS IC. Following this, a low-pass single-pole filter with a low cutoff frequency ($\sim$ 0.03 Hz, to approximate integration) performs continuous-time convolution, enabling an operation similar to matrix-vector multiplication. Sampling the resulting signal with a uniform-sampling scanning circuit, the entire chain is equivalent to multiplication of a discrete-time representation of an EEG signal by a random matrix Φ.

Once the compressively sensed signal from a channel is digitized by an ADC in the CMOS IC, we can reconstruct the original EEG signal as though it were Nyquist sampled. However, in practice, L1-norm minimization is computationally intensive, even for an embedded CMOS IC [37]. Further, because we are ultimately interested in features of the EEG for subsequent inference operations, we can focus on efficient methods for feature extraction rather than full signal

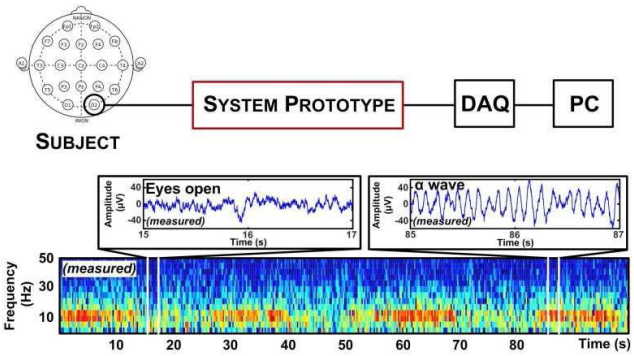

Fig. 20. Setup and measured results of EEG acquisition from a human subject [12].

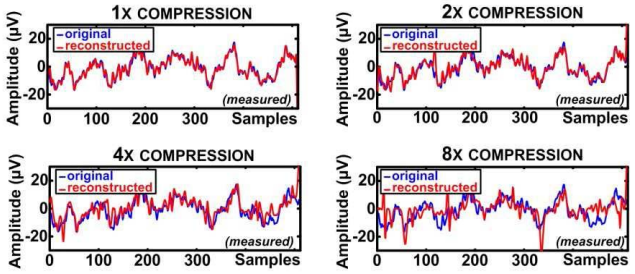

Fig. 21. Reconstructed EEG signals for various compression factors from measured samples [12].

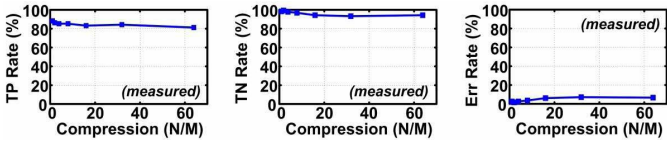

Fig. 22. Measured classification results for seizure detection, including TP (true positive), TN (true negative) and the error rate [12].

reconstruction. Specifically, a common feature set for EEG is the spectral energy distribution of each channel (e.g., over a 1–2 s epoch). Such features can be obtained through a bank of band-pass filters (with appropriately chosen center frequencies and bandwidths) followed by energy accumulation. The key to our algorithmic approach is that energy accumulation of a vector can be achieved by taking its inner product with itself, and that inner products between vectors are preserved following random projection [40]. With our interest being to accurately estimate inner-products rather than the original signal, sparse reconstruction, and thus L1-norm minimization, can be avoided. Instead, much simpler L2-norm minimization can be performed to estimate the signal, simply so that a band-pass filter with desired frequency response (center frequency and bandwidth) can be applied. This leads to a simple linear projection to estimate $\vec{x}$:

$$\tilde{x} = \Phi^T(\Phi\Phi^T)^{-1}\vec{y}. \tag{6}$$

As an example, for this case study, we demonstrate how the resulting features can be used to perform seizure detection in epileptic patients. System demonstration details are given in the next section.

C. System Demonstration

To demonstrate the system prototype, EEG acquisition is performed recording α-waves from a human subject using standard Ag/AgCl electrodes. Fig. 20 shows the setup used. Two electrodes feed into the thin-film low-noise amplifier, one which is connected to the occipital location and one which is a reference electrode connected on the apex. During acquisition, the subject cycles through 10 s periods of closing and 10 s periods of opening the eyes. From the short-time Fourier transform shown in Fig. 20, the expected 10 Hz rhythm of the α-wave is observed when the subjects eyes are closed.

We also demonstrate compressed EEG acquisition, which includes use of the TFT sub-Nyquist scanning circuits. The setup is similar to that used to acquire EEGs from a human subject. The main difference is that instead of using scalp-interfaced electrodes, a function generator is used for analog replay of EEG data from an epileptic patient. The EEG data for this test is obtained from the CHB-MIT database [41], [42], and the function-generator output is appropriately scaled to the corresponding EEG amplitudes. Fig. 21 shows representative examples of reconstructed EEG waveforms acquired compressively at up to 8× below the Nyquist rate.

We also tested the performance of our system when detecting seizures. The feature vector consisted of 56 different spectral-energy features, extracted from a two second time segment of reconstructed EEG-channel signals [via (6)]. In total, seven EEG channels were included and eight spectral-energy features were extracted from each using band-pass filters centered at frequencies from 0–21 Hz. The EEG data came from a dataset consisting of 4950 non-seizure epochs and 100 seizure epochs, randomly sampled from one epileptic patient from the CHB-MIT database. Seizure detection was carried out using a support-vector machine (SVM) classifier with a radial-basis function (RBF) kernel. As shown in Fig. 22, good performance is maintained even at high compression ratios.

V. Conclusion

We have demonstrated through two case studies how a hybrid architecture, based on leveraging the complementary strengths of LAE and CMOS, is a compelling platform for the next generation of HCIs. For the source separation system we showed how, by exploiting the spatial filter capabilities of a large-area microphone array, we are able to successfully isolate the voices of two simultaneous speakers. This could ultimately be used as an alternative to a close contact microphone, as a front-end for a voice-command recognition system, or as a sound-source location detector. Similarly, for the EEG system we demonstrated how by combining electrodes and thin-film circuits on the same flexible sheet, we developed a system with a more natural form-factor and a reduced number of external interfaces. This improves patient comfort and facilitates deployment outside of a clinical setting. Additionally, we showed how by incorporating compressed sensing and SVM classifiers, this system goes beyond just

providing raw EEG reading, and can also perform specific inferences, such as seizure detection. Both cases highlight the importance of signal-processing/-inference algorithms, in two regards. The first is for converting embedded signals, which only peripherally express human intentions and/or states of interest, but which can be opportunistically acquired by LAE sensors, into specific outputs for controlling HCIs of the future. The second is for overcoming the performance limitations of LAE in order to robustly obtain the specific control outputs.

REFERENCES

[1] G. Werner-Allen *et al.*, "Deploying a wireless sensor network on an active volcano," *IEEE Internet Comput.*, vol. 10, no. 2, pp. 18–25, Mar./Apr. 2006.

[2] Applied Materials, Inc. (May 2016). *AKT-PECVD System for TFT-LCD*. [Online]. Available: http://www.appliedmaterials.com/products/akt-pecvd-system-for-tft-lcd

[3] W. S. A. Rieutort-Louis *et al.*, "Integrating and interfacing flexible electronics in hybrid large-area systems," *IEEE Trans. Compon., Packag. Manuf. Technol.*, vol. 5, no. 9, pp. 1219–1229, Sep. 2015.

[4] J. Shah, "Strain sensivity of thick-film resistors," *IEEE Trans. Compon., Hybrids, Manuf. Technol.*, vol. 3, no. 4, pp. 554–564, Dec. 1980.

[5] L. Zhou, S. Jung, E. Brandon, and T. N. Jackson, "Flexible substrate micro-crystalline silicon and gated amorphous silicon strain sensors," *IEEE Trans. Electron Devices*, vol. 53, no. 2, pp. 380–385, Feb. 2006.

[6] H. Wang, L. Chen, J. Wang, Q. Sun, and Y. Zhao, "A micro oxygen sensor based on a nano sol-gel TiO_2 thin film," *Sensors*, vol. 14, no. 9, p. 16423–16433, Sep. 2014.

[7] C. Dagdeviren *et al.*, "Conformable amplified lead zirconate titanate sensors with enhanced piezoelectric response for cutaneous pressure monitoring," *Nature Commun.*, vol. 5, no. 4496, pp. 1–10, Aug. 2014.

[8] Y. M. Chi, T.-P. Jung, and G. Cauwenberghs, "Dry-contact and noncontact biopotential electrodes: Methodological review," *IEEE Rev. Biomed. Eng.*, vol. 3, pp. 106–119, Oct. 2010.

[9] N. Verma *et al.*, "Enabling scalable hybrid systems: Architectures for exploiting large-area electronics in applications," *Proc. IEEE*, vol. 103, no. 4, pp. 690–712, Apr. 2015.

[10] J. Sanz-Robinson *et al.*, "Large-area microphone array for audio source separation based on a hybrid architecture exploiting thin-film electronics and CMOS," *IEEE J. Solid-State Circuits*, vol. 51, no. 4, pp. 979–991, Apr. 2016.

[11] J. Sanz-Robinson *et al.*, "Robust blind source separation in a reverberant room based on beamforming with a large-aperture microphone array," in *Proc. IEEE Int. Conf. Acoust., Speech Signal Process. (ICASSP)*, Mar. 2016, pp. 440–444.

[12] T. Moy *et al.*, "An EEG acquisition and biomarker-extraction system using low-noise-amplifier and compressive-sensing circuits based on flexible, thin-film electronics," *IEEE J. Solid-State Circuits*, to be published.

[13] Y. Hu *et al.*, "3D Gesture-sensing system for interactive displays based on extended-range capacitive sensing," in *IEEE Int. Solid-State Circuits Conf. Dig. Tech. Papers (ISSCC)*, Feb. 2014, pp. 212–213.

[14] W. Rieutort-Louis, T. Moy, Z. Wang, S. Wagner, J. C. Sturm, and N. Verma, "A large-area image sensing and detection system based on embedded thin-film classifiers," *IEEE J. Solid-State Circuits*, vol. 51, no. 1, pp. 281–290, Jan. 2016.

[15] Y. Hu *et al.*, "Large-scale sensing system combining large-area electronics and CMOS ICs for structural-health monitoring," *IEEE J. Solid-State Circuits*, vol. 49, no. 2, pp. 513–523, Feb. 2014.

[16] Y. Hu *et al.*, "A self-powered system for large-scale strain sensing by combining CMOS ICs with large-area electronics," *IEEE J. Solid-State Circuits*, vol. 49, no. 4, pp. 838–850, Apr. 2014.

[17] L. Huang *et al.*, "A super-regenerative radio on plastic based on thin-film transistors and antennas on large flexible sheets for distributed communication links," in *IEEE Int. Solid-State Circuits Conf. Dig. Tech. Papers (ISSCC)*, Feb. 2013, pp. 458–459.

[18] L. L. Beranek and T. J. Mellow, *Acoustics: Sound Fields and Transducers*. San Francisco, CA, USA: Academic, 2012, pp. 202–205.

[19] R. L. Freeman, *Fundamentals of Telecommunications*. New York, NY, USA: Wiley, 2005, pp. 90–91.

[20] H. Gleskova and S. Wagner, "Amorphous silicon thin-film transistors on compliant polyimide foil substrates," *IEEE Electron Device Lett.*, vol. 20, no. 9, pp. 473–475, Sep. 1999.

[21] J. Benesty, M. Sondhi, and Y. Huang, *Springer Handbook of Speech Processing*. New York, NY, USA: Springer-Verlag, 2008, pp. 1023–1029.

[22] H. Kuttruff, "On the audibility of phase distortions in rooms and its significance for sound reproduction and digital simulation in room acoustics," *Acta Acustica United Acustica*, vol. 74, no. 1, pp. 3–5, Jun. 1991.

[23] J. M. Sachar, H. F. Silverman, and W. R. Patterson, "Microphone position and gain calibration for a large-aperture microphone array," *IEEE Trans. Speech Audio Process.*, vol. 13, no. 1, pp. 42–52, Jan. 2005.

[24] S. Rickard and O. Yilmaz, "On the approximate W-disjoint orthogonality of speech," in *Proc. IEEE Int. Conf. Acoust., Speech, Signal Process. (ICASSP)*, vol. 1. May 2002, pp. I-529–I-532.

[25] C. M. Bishop, *Pattern Recognition and Machine Learning*. Springer, 2006, pp. 423–427.

[26] P. J. Rousseeuw, "Silhouettes: A graphical aid to the interpretation and validation of cluster analysis," *J. Comput. Appl. Math.*, vol. 20, no. 1, pp. 53–65, 1987.

[27] P. Kabal, "TSP Speech database," Dept. Elect. Comput. Eng., McGill Univ., Montreal, QC, Canada, Tech. Rep., Sep. 2002.

[28] A. W. Rix, J. G. Beerends, M. P. Hollier, and A. P. Hekstra, "Perceptual evaluation of speech quality (PESQ)—A new method for speech quality assessment of telephone networks and codecs," in *Proc. IEEE Int. Conf. Acoust., Speech, Signal Process. (ICASSP)*, vol. 2. May 2001, pp. 749–752.

[29] K. Ramadan, D. Sameoto, and S. Evoy, "A review of piezoelectric polymers as functional materials for electromechanical transducers," *Smart Mater. Struct.*, vol. 23, no. 3, p. 033001, Jan. 2014.

[30] V. Trees and L. Harry, *Optimum Array Processing: Part IV Detection, Estimation, and Modulation Theory*. New York, NY, USA: Wiley, 2002, p. 66.

[31] M. A. Richards, *Fundamentals of Radar Signal Processing*. New York, NY, USA: McGraw-Hill, 2014. [Online]. Available: http://users.ece.gatech.edu/mrichard/NoncoherentIntegrationGainApproximations.pdf

[32] S. Wagner *et al.*, "Investigating the architecture of flexible large-area hybrid systems," *Soc. Inf. Display (SID)*, vol. 31, no. 4, pp. 12–17, Jul. 2015.

[33] R. Horlings, D. Datcu, and L. J. M. Rothkrantz, "Emotion recognition using brain activity," in *Proc. 9th Int. Conf. Comput. Syst.*, Jun. 2008, p. 6.

[34] K. LaFleur, K. Cassady, A. Doud, K. Shades, E. Rogin, and B. He, "Quadcopter control in three-dimensional space using a noninvasive motor imagery-based brain–computer interface," *J. Neural Eng.*, vol. 10, no. 4, p. 046003, Jun. 2013.

[35] C. C. Enz and G. C. Temes, "Circuit techniques for reducing the effects of op-amp imperfections: Autozeroing, correlated double sampling, and chopper stabilization," *Proc. IEEE*, vol. 84, no. 11, pp. 1584–1614, Nov. 1996.

[36] T. Moy *et al.*, "Thin-film circuits for scalable interfacing between large-area electronics and CMOS ICs," in *Proc. 72nd Annu. Device Res. Conf.*, Jun. 2014, pp. 271–272.

[37] R. G. Baraniuk, "Compressive sensing," *IEEE Signal Process. Mag.*, vol. 24, pp. 118–124, Jul. 2007.

[38] A. M. Abdulghani, A. J. Casson, and E. Rodriguez-Villegas, "Compressive sensing scalp EEG signals: Implementations and practical performance," *Med. Biol. Eng. Comput.*, vol. 50, no. 11, pp. 1137–1145, Nov. 2012.

[39] S. Kirolos *et al.*, "Analog-to-information conversion via random demodulation," in *Proc. IEEE Dallas/CAS Workshop Design, Appl., Integr., Softw.*, Oct. 2006, pp. 71–74.

[40] R. Hecht-Nielsen, "Context vectors: General purpose approximate meaning representations self-organized from raw data," in *Proc. Comput. Intell., Imitating Life*, 1994, pp. 43–56.

[41] A. L. Goldberger *et al.*, "PhysioBank, PhysioToolkit, and PhysioNet: Components of a new research resource for complex physiologic signals," *Circulation*, vol. 101, no. 23, pp. e215–e220, Jun. 2000.

[42] PhysioNet. (May 2016). *CHB-MIT Scalp EEG Database*. [Online]. Available: https://www.physionet.org/pn6/chbmit/

Josue Sanz-Robinson received the B.Eng. degree in electrical engineering (Hons.) from McGill University, Montreal, Canada in 2010, and the M.A. and Ph.D. degrees in Electrical Engineering in 2012 and 2016, respectively, both from Princeton University, Princeton, NJ, USA. Dr. Sanz-Robinson was a recipient of a 2013 Qualcomm Innovation Fellowship.

Currently, he is a Research Scientist at Pindrop Security. His research focuses on developing data mining techniques for large audio datasets, primarily applied to detecting financial fraud over the phone channel.

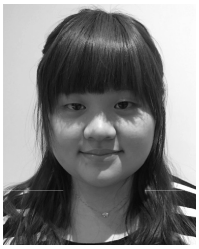

Tiffany Moy received the B.S.E. (magna cum laude) and M.A. degrees in electrical engineering from Princeton University, Princeton, NJ in 2012 and 2014, respectively. She is currently pursuing the Ph.D. degree in electrical engineering at Princeton University. Her research interests include thin-film circuits and algorithms for hybrid large-area electronics/CMOS system design.

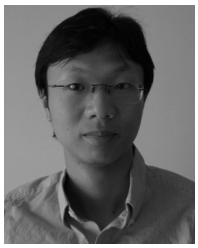

Liechao Huang (S'12) received the B.S. degree in Microelectronics from Fudan University, Shanghai, China in 2010, and the M.A. and Ph.D. degrees in Electrical Engineering in 2012 and 2016, respectively, both from Princeton University, Princeton, NJ, USA. His research interests include thin-film circuit design for power, radio and sensing interfaces, CMOS analog and mixed signal design for sensing interfaces and power management and hybrid system design combining thin-film circuits and CMOS ICs.

Dr. Huang is the recipient of Princeton Engineering Fellowship and Gordon Wu award at Princeton University.

Warren Rieutort-Louis (S'12–M'15) received the B.A. (Hons.) and M.Eng. degrees in electrical and information engineering from Trinity College, Cambridge University, Cambridge, U.K., in 2009, and the M.A. and Ph.D. degrees in Electrical Engineering in 2012 and 2015, respectively, both from Princeton University, Princeton, NJ, USA.

He was a Graduate Teaching Fellow with Princeton McGraw Center for Teaching and Learning. His research interests include thin-film materials, processes, devices, and circuits for large-area electronic systems. Dr. Rieutort-Louis was the recipient of the IBM Ph.D. Fellowship, the Andlinger Center Maeder Fellowship in Energy and the Environment, and the Princeton Harold W. Dodds Honorific Fellowship.

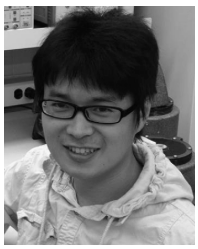

Yingzhe Hu received the B.S. degrees in both Physics and Microelectronics from Peking University, and the M.A. and Ph.D. degrees in Electrical Engineering from Princeton University in 2011 and 2015 respectively. His research focuses on flexible electronics and CMOS IC hybrid sensing system design and capacitive 3D gesture sensing system design. Dr. Hu is the recipient of 2013 Qualcomm Innovation Fellowship, Gordon Wu award at Princeton University, 2013 ISSCC SRP award and 2013 VLSI best student paper award.

Sigurd Wagner (SM'78–F'00) received his Ph.D. from the University of Vienna, Vienna, Austria. Following a Post-Doctoral Fellowship at Ohio State University, he worked from 1970 to 1978 at the Bell Telephone Laboratories in Murray Hill and Holmdel, New Jersey, on semiconductor memories and heterojunction solar cells. He then joined the Solar Energy Research Institute (now NREL), in Golden, CO, as the founding Chief of the Photovoltaic Research Branch. Since 1980, he has been Professor of Electrical Engineering at Princeton University; in 2015 he became Professor Emeritus and Senior Scholar. He has been developing fundamentally new materials, processes, and components for flexible large-area electronics, electrotextiles, and electronic skin, and is considered the father of soft elastic electronics. He is a member of Princeton's Large-area Systems Group whose goal is to demonstrate complete large-area applications based on hybrid thin film / CMOS architectures. Dr. Wagner is a fellow of the American Physical Society and a Member of the Austrian Academy of Science. He received the Nevill Mott Prize for his groundbreaking research, both fundamental and applied, on amorphous semiconductors and chalcopyrites, and the ITC Anniversary Prize for pioneering research on flexible and stretchable large-area electronics, and the comprehensive study of its mechanical behavior.

James C. Sturm (S'81–M'85–SM'95–F'01) was born in Berkeley Heights, NJ, in 1957. He received the B.S.E. degree in electrical engineering and engineering physics from Princeton University, Princeton, NJ, in 1979 and the M.S.E.E. and Ph.D. degrees in 1981 and 1985, respectively, both from Stanford University, Stanford, CA. In 1979, he joined Intel Corporation, Santa Clara, CA, as a Microprocessor Design Engineer, and in 1981 he was a Visiting Engineer at Siemens, Munich, Germany. In 1986, he joined the faculty of Princeton University, where he is currently the Stephen R. Forrest Professor in Electrical Engineering. From 1998 to 2015, he was the director of the Princeton Photonics and Optoelectronic Materials Center (POEM) and its successor, the Princeton Institute for the Science and Technology of Materials (PRISM). In 1994-1995, he was a von Humboldt Fellow at the Institut fuer Halbleitertechnik at the University of Stuttgart, Stuttgart, Germany. He has worked in the fields of silicon-based heterojunctions, thin-film and flexible electronics, photovoltaics, the nano-bio interface, three-dimensional (3-D) integration, and silicon-on-insulator.

Dr. Sturm is a fellow of IEEE. He has won over ten awards for teaching excellence and was a National Science Foundation Presidential Young Investigator. In 1996 and 1997, he was the technical program chair and general chair of the IEEE Device Research Conference, respectively. He served on the organizing committee of IEDM (1988 to 1992 and 1998 to 1999), having chaired both the solid-state device and detectors/sensors/displays committees. He has served on the boards of directors of the Materials Research Society and the Device Research Conference, and co-founded Aegis Lightwave and SpaceTouch.

Naveen Verma received the B.A.Sc. degree in Electrical and Computer Engineering from the University of British Columbia, Vancouver, Canada in 2003, and the M.S. and Ph.D. degrees in Electrical Engineering from Massachusetts Institute of Technology in 2005 and 2009 respectively. Since July 2009 he has been with the department of Electrical Engineering at Princeton University, where he is currently an Associate Professor. His research focuses on advanced sensing systems, including low-voltage digital logic and SRAMs, low-noise analog instrumentation and data-conversion, large-area sensing systems based on flexible electronics, and low-energy algorithms for embedded inference, especially for medical applications. Prof. Verma is recipient or co-recipient of the 2006 DAC/ISSCC Student Design Contest Award, 2008 ISSCC Jack Kilby Paper Award, 2012 Alfred Rheinstein Junior Faculty Award, 2013 NSF CAREER Award, 2013 Intel Early Career Award, 2013 Walter C. Johnson Prize for Teaching Excellence, 2013 VLSI Symp. Best Student Paper Award, and 2014 AFOSR Young Investigator Award.